

Ambient Contrast Ratio of a Liquid Crystal Cell Stacked on a Luminescent Layer

Yoshiki Yamada, Yasuhiro Tsutsumi, Ichiro Fujieda

fujieda@se.ritsumei.ac.jp

Ritsumeikan University, 1-1-1 Noji-Higashi, Kusatsu, Shiga 525-8577, Japan

Keywords: ambient contrast ratio, liquid crystal, luminescent waveguide

ABSTRACT

A twisted-nematic liquid crystal cell was placed on a Coumarin 6 layer formed on a transparent plate. Its ambient contrast ratio remained around 10 even at the illuminance of 222 klx while that of a transmissive liquid crystal display operated at 397 cd/m² decreased to 5.4.

1 INTRODUCTION

Ambient contrast ratio (ACR) is regarded as one of the key parameters for a liquid crystal display (LCD) and an organic light-emitting diode display (OLED) [1]. Indeed, visibility under the sun and low power consumption are highly desired for mobile applications. To maintain readability in bright environments, one can increase the luminance of an emissive display such as a transmissive LCD and an OLED. Inevitably, its power consumption increases. Reducing scattering improves the visibility of a transmissive LCD [2]. This approach is an alleviation rather than a fundamental solution. In this regard, reflective LCDs and transfective LCDs are unique in a sense that they utilize ambient light to display images [3]. Unfortunately, this very fact results in an unstable color gamut because the chromaticity coordinates of the three primary colors depend on the lighting condition. More seriously, it is rather small: for example, 19 % coverage of the NTSC standard is reported for a reflective LCD in 2019 [4]. Luminescent materials can provide a wide and stable color gamut as we know from our experiences in plasma displays. Other previous studies on the use of these materials for display applications include guest-host systems for a twisted-nematic (TN) LCD [5] as well as for a cholesteric LCD [6], a laser phosphor display [7], a transparent phosphor screen [8], and energy-harvesting projectors [9-11]. For mobile applications, one can harvest energy from ambient light by stacking an LC panel on a luminescent layer with a waveguiding structure [12].

In this paper, we consider using luminescent materials for solving the trade-off between the readability of a display and its power consumption in bright environments.

2 THEORY

Let us model the ACR for the configuration illustrated in Fig. 1. Suppose that ambient light of irradiance I_a [W/m²] and normalized spectrum $S_a(\lambda)$ [photons/nm] is incident on the LC cell at a certain angle θ_{in} . It is scattered

at the surface as well as inside with a certain probability P_{sc} . A fraction of this scattered light $P_{sc}I_a$ reaches the observer. When the LC cell is set to black state, the ambient light does not reach the luminescent layer. Denoting the luminous efficacy and luminous efficiency function as K and $V(\lambda)$, respectively, the luminance [cd/m²] is expressed for the black state as follows.

$$L_B = \frac{P_{sc}I_a}{4\pi} K \int S_a(\lambda) V(\lambda) d\lambda \quad (1)$$

When the LC cell is set to white state, the transmitted ambient light excites the luminescent layer. Denoting the transmittance as $T_{LC}(\theta_{in})$, the radiant exitance of the photoluminescence (PL) photons emitted by this layer I_{PL} [W/m²] is given by $\eta T_{LC}(\theta_{in})I_a$, where η is the quantum efficiency of this layer. The PL photons need to pass through the LC cell to reach the observer. This probability is given by $T_{LC}(\theta_{obs})$ where θ_{obs} specifies the direction of observation. The scattered component $P_{sc}I_a$ exists irrespective of the state of the LC cell. Therefore, denoting the normalized emission spectrum of this layer as $S_{PL}(\lambda)$, the luminance for the white state is given by,

$$L_W = L_B + \frac{T_{LC}(\theta_{obs})\eta T_{LC}(\theta_{in})I_a}{4\pi} K \int S_{PL}(\lambda) V(\lambda) d\lambda \quad (2)$$

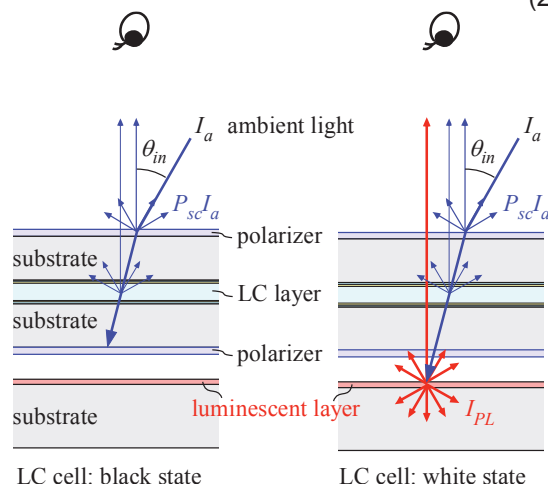


Fig. 1 Ambient light is utilized for displaying an image by stacking an LC cell on a luminescent layer.

The definition of ACR is L_w / L_b . Substituting the equations above, it is expressed as,

$$ACR = 1 + \frac{T_{LC}(\theta_{obs})\eta T_{LC}(\theta_{in}) \int S_{PL}(\lambda)V(\lambda)d\lambda}{P_{sc} \int S_a(\lambda)V(\lambda)d\lambda}. \quad (3)$$

Because the term I_a cancels out in Eq. (3), ACR does not depend on it. Hence, we expect good visibility even at an extremely high level of illuminance. Readability under dark can be secured by exciting the luminescent layer with an external backlight unit.

In case of a transmissive LCD, the term $\eta T_{LC}(\theta_{in})I_a$ in Eq. (2) is replaced by I_{BLU} , the radiant exitance of a backlight unit. Note that the transmittance T_{LC} depends on the wavelength due to the color filters inside the LC panel. Denoting the normalized spectrum of the backlight unit as $S_{BLU}(\lambda)$, the ACR for a transmissive LCD is given by,

$$ACR = 1 + \frac{I_{BLU} \int T_{LC}(\theta_{obs}, \lambda) S_{BLU}(\lambda) V(\lambda) d\lambda}{P_{sc} I_a \int S_a(\lambda) V(\lambda) d\lambda}. \quad (4)$$

As the ambient light irradiance I_a increases, ACR approaches unity and the LCD becomes unreadable.

3 EXPERIMENT

3.1 Fabrication

A solution of 0.07 wt% luminescent dye (Sigma Aldrich, Coumarin 6) in ultra-violet curable resin (Norland Products, NOA81) was spun coated on a 50 x 50 x 5 mm acrylic plate at 2000 rpm and cured. This film-forming process was repeated six times to increase the absorbance at 450 nm to 0.93. Its photograph is shown in Fig. 2. We call this component a luminescent waveguide (LWG) in this paper.

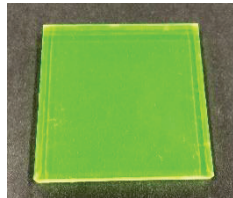


Fig. 2 Photograph of an LWG taken under room light.

A TN-LC cell was adopted in this study because the materials and components to fabricate one were readily available to us: an empty cell (E. H. C. Co. Ltd, KSRT-05/B111P1NSS05), a nematic LC material (Merck, MLC-3018) and polarizer films. The cell had two 1.1 mm-thick glass substrates with a 5 μ m-thick gap. It had a 10 mm x 10 mm active area where two transparent electrodes applied bias to the LC layer through alignment layers. When a $\pm 5V$ square-wave voltage was applied at 60 Hz, the transmittance of this cell was measured to be 0.000493. Under zero bias, it was 0.445 so that the maximum contrast ratio of this LC cell alone was 904.

3.2 Measurement

The LWG was placed on a black sheet of paper and the TN-LC cell was stacked on it without any index-matching oil. As shown in Fig. 3, a flashlight (ThruNite, Model TN50) was placed 350 mm away. The diffuse light from its white LEDs illuminated the device at $\theta_{in} = 30^\circ$. Its power was set to five different levels and illuminance was measured each time. A monochrome camera (The Imaging Source, Model DMK33UX249) was placed 95 mm away. It acquired the image of the TN-LC cell for each setting of the illuminance with 12-bit analog-to-digital conversion resolution. At high illuminance settings, a black sheet of paper was placed around the camera to shield the heat from the flashlight (not shown in Fig. 3).

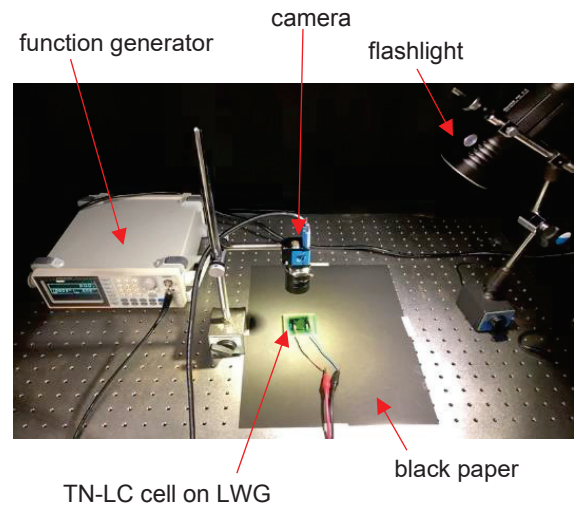


Fig. 3 Setup for the ACR measurement.

Example images are shown in Fig. 4. A region of interest is set in the active area of the cell in each image. Average pixel values were extracted from these regions and ACR was calculated.

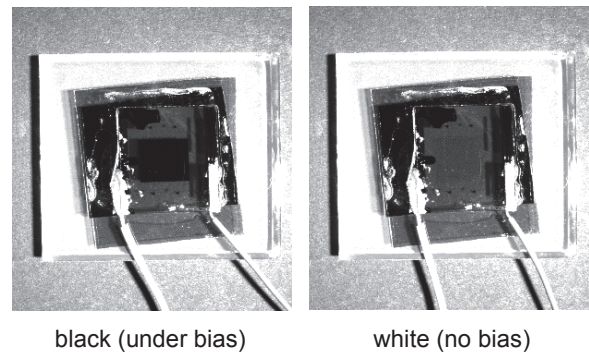


Fig. 4 Example images acquired by the camera.

This ACR measurement was repeated with a smartphone (Apple, iPhone 8 Plus). Its transmissive LCD displayed a green image at three different luminance levels which were measured before being illuminated with the flashlight.

The measured ACR is compared in Fig. 5. The curves are for guiding eyes only. The solid circles marked as “LC+LWG” represent the result for the TN-LC cell stacked on the LWG. Its ACR remains at around 10 even at the highest illuminance in this experiment (222 klx). This behavior is consistent with Eq. (3). Other markers in Fig. 5 show the results for the transmissive LCD operated at three luminance levels as indicated. As expected from Eq. (4), its ACR decreases monotonically with the illuminance. For example, it is 5.4 at 222 klx when the luminance is 397 cd/m².

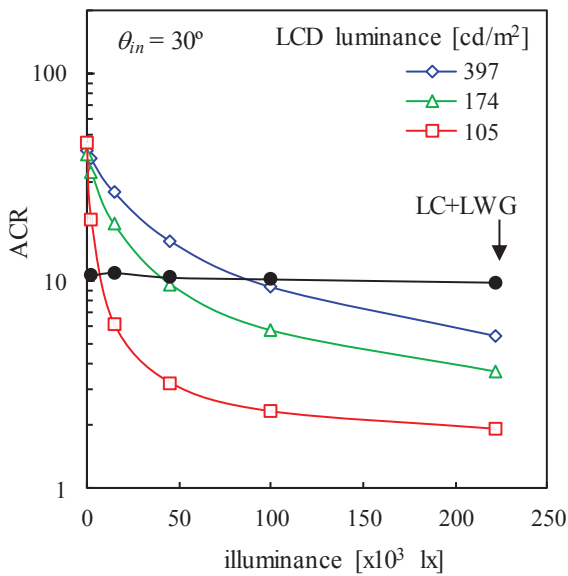


Fig. 5 Comparison of the proposed configuration (LC cell on LWG) and a transmissive LCD.

3.3 Further measurement

A display is often illuminated obliquely. To simulate this observation condition, an LED flashlight (HeliusSuper, Model Omega X) was moved on an arc so that the device (TN-LC cell on LWG) was illuminated obliquely. As shown in Fig. 6, a cylinder made of a black paper was inserted to limit the angular range of the light from the flashlight. The cylinder was 210 mm-long and its diameter was 57 mm. The distance between its tip and the device was 50 mm. This flashlight had smaller power than the previous one. The illuminance was measured for each setting for the illumination direction and the power of the flashlight.

As shown in Fig. 7, the measured ACR decreases monotonically with the illumination direction. This behavior might be attributed to $T_{LC}(\theta_m)$ in Eq. (3): it is smaller at a larger θ_m and the luminescent layer is less

excited. The illuminance decreases with θ_m because the projected area increases. The ACR measured at a fixed θ_m is constant within the measurement error. Again, this is consistent with Eq. (3).

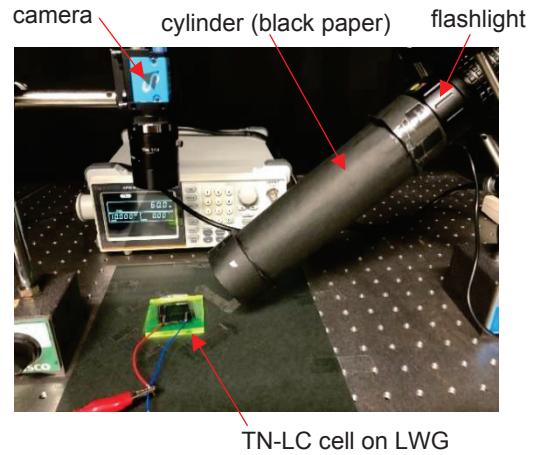


Fig. 6 ACR measurement under the illumination with a narrower angular range.

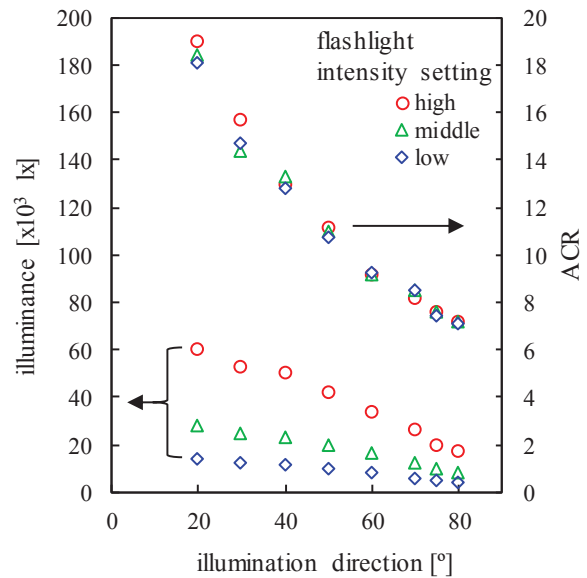


Fig. 7 Dependency on the illumination direction.

4 Discussion

Note that the ACR at 30° in Fig. 7 is about 15. For the case of the more divergent illumination condition in Fig. 3, this value is about 10 as shown in Fig. 5. The discrepancy is caused by the different illumination condition: the angular range of the light incident on the LC cell is smaller due to the black cylinder for the setup in Fig. 6. It would be necessary to control the divergence of the ambient light for a rigorous result. Hence, a standard procedure such as one reported for e-papers [13] is desired for ACR measurement.

Visibility under oblique illumination would improve by adopting other LC modes such as in-plane switching (IPS) and multi-domain vertical alignment (MVA).

The luminescent layer was 1.1 mm away from the LC layer in this experiment. This would cause parallax error in many applications. Embedding luminescent materials in the pixels of an LC panel will eliminate this error. The process developed for the color conversion layers in OLEDs might be adopted to fabricate such an in-cell structure. An in-cell polarizer [14] is also required for common LC modes. Although its fabrication might be more challenging, there is a continuing interest for developing one to improve contrast ratio of an LCD [15].

Finally, it is worth noting that majority of the PL photons are trapped in the LWG via total internal reflection (TIR). For the case of isotropic emission, this probability is equal to $\cos\theta_c$ where θ_c is the critical angle for TIR. The trapped PL photons can be harvested by placing solar cells at the edge surfaces of the LWG to generate electric power [16].

5 CONCLUSIONS

Ambient contrast ratio was formulated for an LC cell stacked on a luminescent layer. Because the radiant exitance of the PL photons is proportional to the irradiance of the incident light, the ACR of this configuration does not depend on the illuminance. In experiment, a TN-LC cell was placed on the Coumarin 6 layer formed on an acrylic plate. White light from a flashlight was directed to the LC cell at 30° from the plane normal. Indeed, the ACR measured with this setup did not depend on the illuminance and it remained at about 10 even at 222 klx. In contrast, the ACR of a transmissive LCD operated at 397 cd/m² decreased to 5.4 at 222 klx. Next, we limited the angular range of the flashlight and illuminated the TN-LC cell obliquely. The measured ACR decreased monotonically with the illumination direction due to the decrease in the transmittance of the TN-LC cell. The use of other LC modes such as IPS and MVA would increase ACR under oblique illumination.

Embedding luminescent materials in an LC panel and utilizing ambient light can be a solution for the trade-off between the readability of a display in bright environments and its power consumption. A wide color gamut and the potential for energy harvesting are additional advantages over the reflective display technologies.

ACKNOWLEDGEMENTS

We would like to thank Prof. Mitsuhiro Shigeta for helpful discussions.

REFERENCES

[1] H. Chen, J. Lee, B. Lin, S. Chen and S. Wu, "Liquid crystal display and organic light-emitting diode display: present status and future perspectives," *Light Sci. Appl.* **7**, 17168 (2018).
 [2] Y. Kawahira, K. Murata, T. Nakai, M. Hasegawa, A. Sakai, K. Minoura, N. Smith, "Sunlight readable FFS

LCD with high contrast ratio and wide color gamut under high ambient light situations," *Proc. 25th IDW*, 91-94 (2018).

[3] X. Zhu, Z. Ge, T. X. Wu, and S. Wu, "Transflective liquid crystal displays," *J. Disp. Technol.* **1**(1), 15-29 (2005).
 [4] H. Hakoi, M. Ni, J. Hashimoto, T. Sato, S. Shimada, K. Minoura, A. Itoh, K. Tanaka, H. Matsukizono and M. Otsubo, "High-performance and low-power full color reflective LCD for new applications," *SID Symp. Dig. Tech. Pap.* **50**, 279-282 (2019).
 [5] R. Yamaguchi, J. Kishida and S. Sato, "Multicolor switching properties in fluorescent liquid crystal displays," *Jpn. J. Appl. Phys.* **39**, 5235-5238 (2000).
 [6] J. Kim, S. Joo, and J. Song, "Reflective-emissive photoluminescent cholesteric liquid crystal display," *Appl. Opt.* **52**(34), 8280-8286 (2013).
 [7] R. A. Hajjar, "Introducing scalable, freeform, immersive, high-definition laser phosphor displays," *SID Symp. Dig. Tech. Pap.* **43**, 985-988 (2012).
 [8] T. X. Sun, Y. Du, X. Wang, B. Cheng, "A novel emissive projection display (EPD) on fully-transparent phosphor screen," *SID Symp. Dig. Tech. Pap.* **50**, 394-397 (2019).
 [9] I. Fujieda, S. Itaya, M. Ohta, Y. Hirai, T. Kohmoto, "Energy-harvesting laser phosphor display and its design considerations," *J. Photon. Energy* **7**(2), 028001 (2017).
 [10] I. Fujieda, T. Kohmoto, K. Yunoki, M. Shigeta, Y. Tsutsumi, "Fabrication and operation of an energy-harvesting color projector," *SID Symp. Dig. Tech. Pap.* **50**, 394-397 (2019).
 [11] K. Yunoki, R. Matsumura, T. Kohmoto, M. Ohta, Y. Tsutsumi, and I. Fujieda, "Crosstalk and optical efficiency of an energy-harvesting color projector utilizing ceramic phosphors," *Appl. Opt.* **58**(36), 9896-9903 (2019).
 [12] M. Shigeta, I. Fujieda, Y. Tsutsumi, "Proposal of energy-harvesting liquid crystal displays," *Proc. 25th IDW*, 218-221 (2018).
 [13] D. Hertel, "Optical measurement standards for reflective e-paper to predict colors displayed in ambient illumination environments," *Color Res. Appl.* **43**, 907-921 (2018).
 [14] Y. Ukai, T. Ohyama, L. Fennell, Y. Kato, M. Paukshto, P. Smith, O. Yamashita, S. Nakanishi, "Current status and future prospect of in-cell-polarizer technology," *J. Soc. Inf. Disp.* **13**(1), 17-24 (2005).
 [15] H. Chen, G. Tan, M. Li, S. Lee, and S. Wu, "Depolarization effect in liquid crystal displays," *Opt. Express* **25**, 11315-11328 (2017).
 [16] W. H. Weber and J. Lambe, "Luminescent greenhouse collector for solar radiation," *Appl. Opt.* **15**(10), 2299-2300 (1976).